

# **Synergy Effect on Atomic Cluster $M_4$ Supported on $MN_4$ - Graphene ( $M=Fe, Ni$ ) for Hydrogen Evolution Reaction**

Jiake Cui<sup>1</sup>, Xiaojing Liu<sup>1</sup>, Yongxue Wei<sup>1</sup>, Xiangjian Shen\*

<sup>1</sup> Engineering Research Center of Advanced Functional Material Manufacturing of Ministry of Education, Zhengzhou University, Zhengzhou 450001, China,

\* To whom correspondence should be addressed: [xjshen85@zzu.edu.cn](mailto:xjshen85@zzu.edu.cn)

## Table of content

**Table S1:** Binding energies between tetrahedral  $M_4$  clusters and  $MN_4$ -Gr substrates in different configurations.

**Table S2:** Binding energies of  $M_4$  clusters in a planar form supported on  $MN_4$ -Gr substrates.

**Table S3:** Bader charge (BC) of each metal atom and N atom of  $M_4@MN_4$ -Gr model catalysts.

**Figure S1:** The optimized stable structures of the substrates and metal clusters.

**Figure S2:** Three basic configurations of optimized  $M_4@MN_4$ -Gr model catalysts.

**Figure S3:** Final configurations of planar  $M_4$  clusters initially bounded to  $MN_4$ -Gr substrates.

**Figure S4:** Schematic diagram of metal and N atoms labelling.

**Figure S5:** Schematic illustration of different adsorption sites on  $M_4$  clusters supported on  $MN_4$ -Gr substrates.

**Figure S6:** The Gibbs free energies of hydrogen adsorption ( $\Delta G_{H^*}$ ) in implicit solvation model.

**Figure S7:** Configuration diagrams of the HER mechanism on four model catalysts.

**Figure S8:** The free energy diagrams of HER in implicit solvation model.

**Figure S9:** Configuration diagram of two hydrogen atoms adsorbed on the  $M_4@MN_4$ -Gr catalyst.

**Table S1:** The binding energies between tetrahedral  $M_4$  clusters and  $MN_4$ -Gr substrates in different configurations, including Regular-Tetrahedron (RT), Side-Tetrahedron (ST) and Inverted-Tetrahedron (IT), respectively.

Catalyst	$E_b$ /(eV)		
	RT	ST	IT
$Fe_4FeN_4Gr$	2.352	2.233	1.158
$Fe_4NiN_4Gr$	1.292	1.275	1.259
$Ni_4FeN_4Gr$	2.491	2.306	2.315
$Ni_4NiN_4Gr$	1.75	1.590	1.590

**Table S2:** Binding energies of  $M_4$  clusters in a planar form supported on  $MN_4$ -Gr substrates.

Catalyst	$E_b$ /(eV)
Flat- $Fe_4@FeN_4Gr$	2.255
Flat- $Fe_4@NiN_4Gr$	0.845
Flat- $Ni_4@FeN_4Gr$	1.603
Flat- $Ni_4@NiN_4Gr$	0.815

**Table S3:** Bader charge (BC) of each metal atom and N atom of  $M_4@MN_4$ -Gr model catalysts.

$Fe_4@FeN_4$ -Gr		$Fe_4@NiN_4$ -Gr		$Ni_4@FeN_4$ -Gr		$Ni_4@NiN_4$ -Gr	
Element	BC( e )	Element	BC( e )	Element	BC( e )	Element	BC( e )
Fe1	-0.76	Ni1	-0.71	Fe1	-0.88	Ni1	-0.75
Fe2	-0.35	Fe1	-0.32	Ni1	-0.24	Ni2	-0.27
Fe3	0.08	Fe2	0.06	Ni2	-0.22	Ni3	-0.22
Fe4	-0.34	Fe3	-0.32	Ni3	0.11	Ni4	0.11
Fe5	-0.34	Fe4	-0.32	Ni4	-0.23	Ni5	-0.23
N1	1.19	N1	1.2	N1	1.18	N1	1.18
N2	1.13	N2	1.22	N2	1.11	N2	1.19
N3	1.21	N3	1.24	N3	1.18	N3	1.22
N4	1.13	N4	1.04	N4	1.18	N4	1.07

**Figure S1:** The optimized stable structures of the substrates and metal clusters, (a)  $FeN_4$ -Gr, (b)  $NiN_4$ -Gr, (c)  $Fe_4$  cluster, (d)  $Ni_4$  cluster.

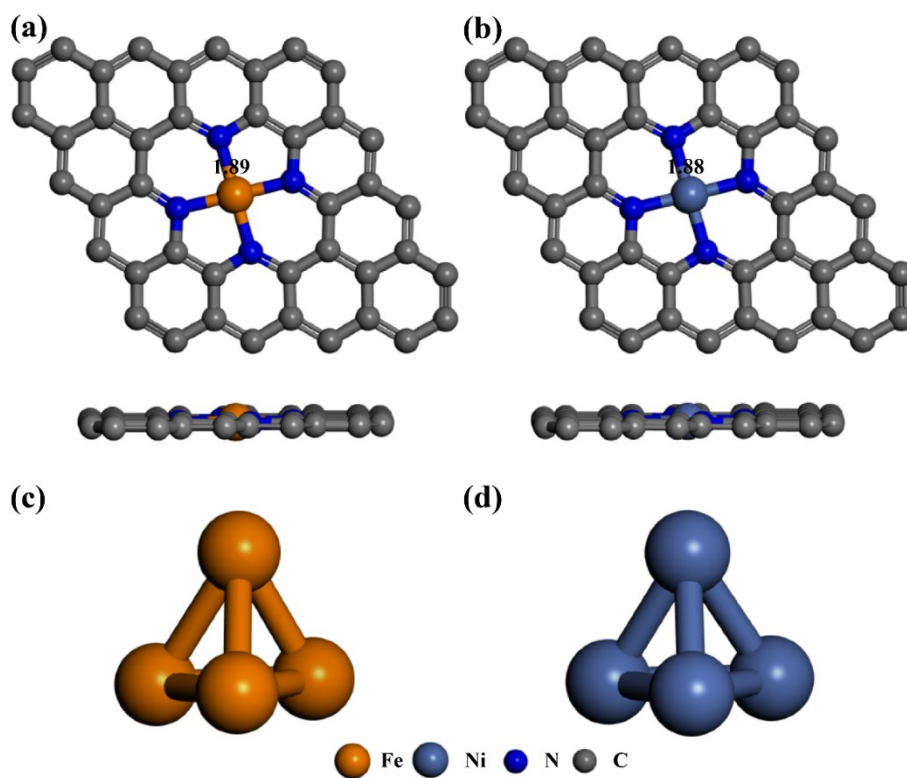
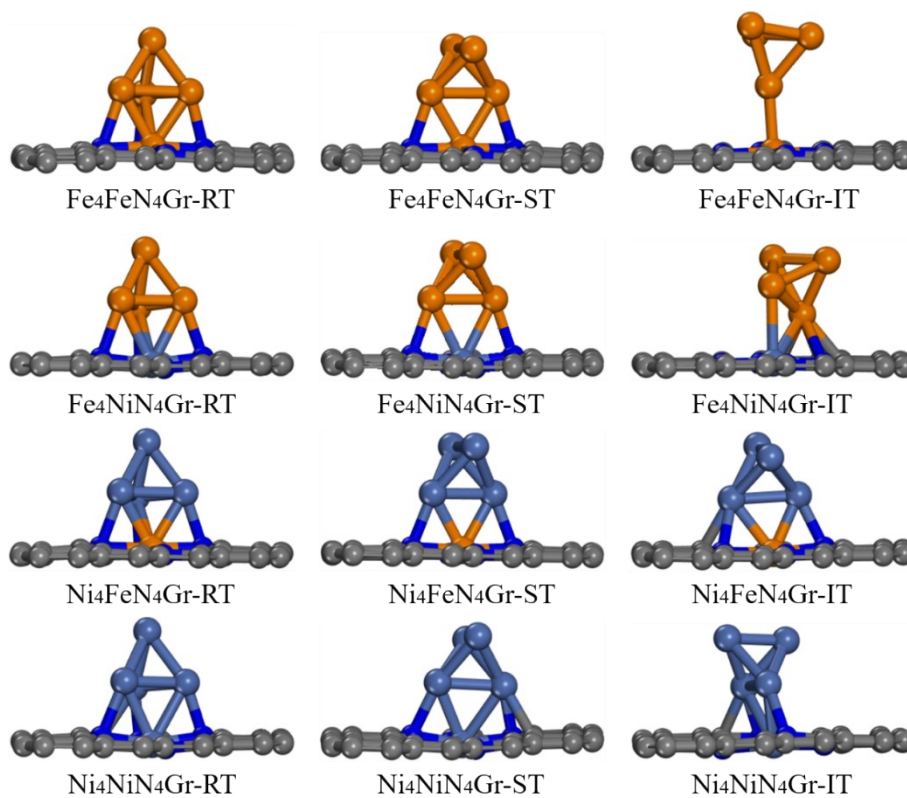


**Figure S2:** Three basic configurations of optimized  $M_4@MN_4$ -Gr model catalysts: Regular-Tetrahedron (RT), Side-Tetrahedron (ST) and Inverted-Tetrahedron (IT).



It can be clearly seen from Figure S2 and Table S1 that the Regular-Tetrahedron is the

most stable in the three configurations, while the Inverted-Tetrahedron tends to be deformed. In the Inverted-Tetrahedron configuration, one vertex atom of the  $M_4$  cluster interacts with the substrate, and the other three atoms are far away from the substrate, which is unstable. When more metal atoms in the  $M_4$  cluster interact with the substrate like Side-Tetrahedron and Regular-Tetrahedron configurations, there will be more electron transfer between the cluster and the substrate, which will make the  $M_4$  cluster stably bind to the  $MN_4$ -Gr substrate.

**Figure S3:** Final configurations of planar  $M_4$  clusters initially bounded to  $MN_4$ -Gr substrates. (a)-(d) are shown for  $Fe_4@FeN_4Gr$ ,  $Fe_4@NiN_4Gr$ ,  $Ni_4@FeN_4Gr$  and  $Ni_4@NiN_4Gr$ , respectively.

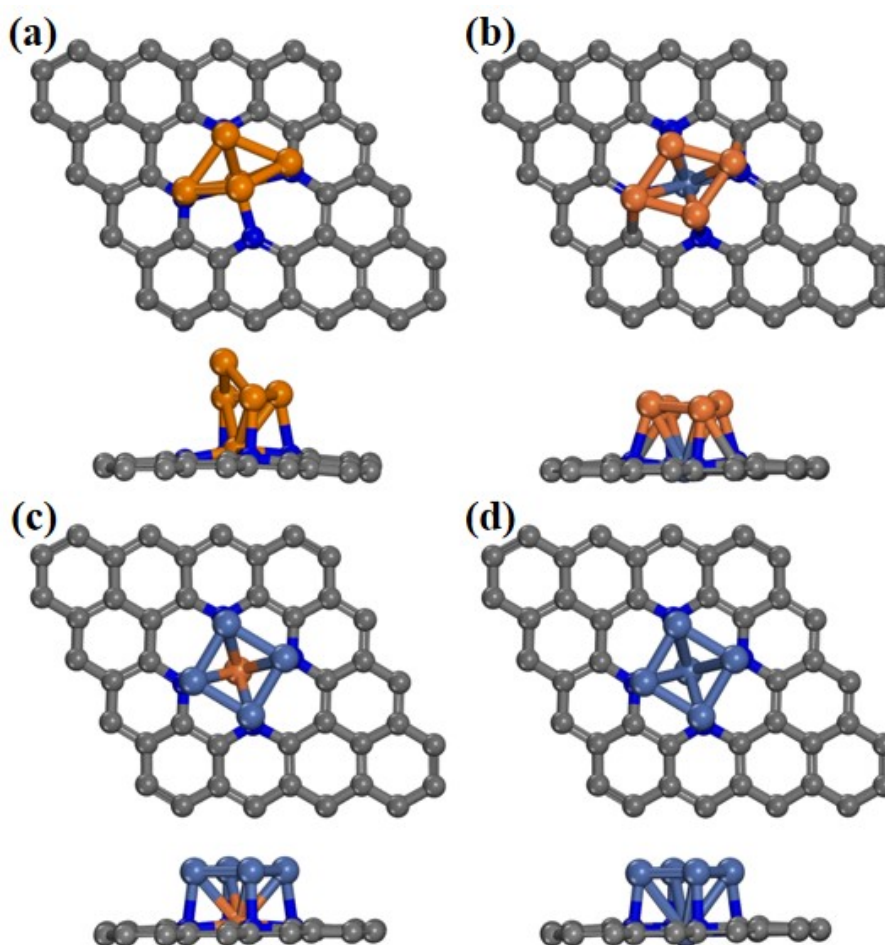


**Figure S4:** Schematic diagram of metal and N atoms labelling: (a)-(d) are shown for  $Fe_4FeN_4Gr$ ,  $Fe_4NiN_4Gr$ ,  $Ni_4FeN_4Gr$  and  $Ni_4NiN_4Gr$ , respectively.

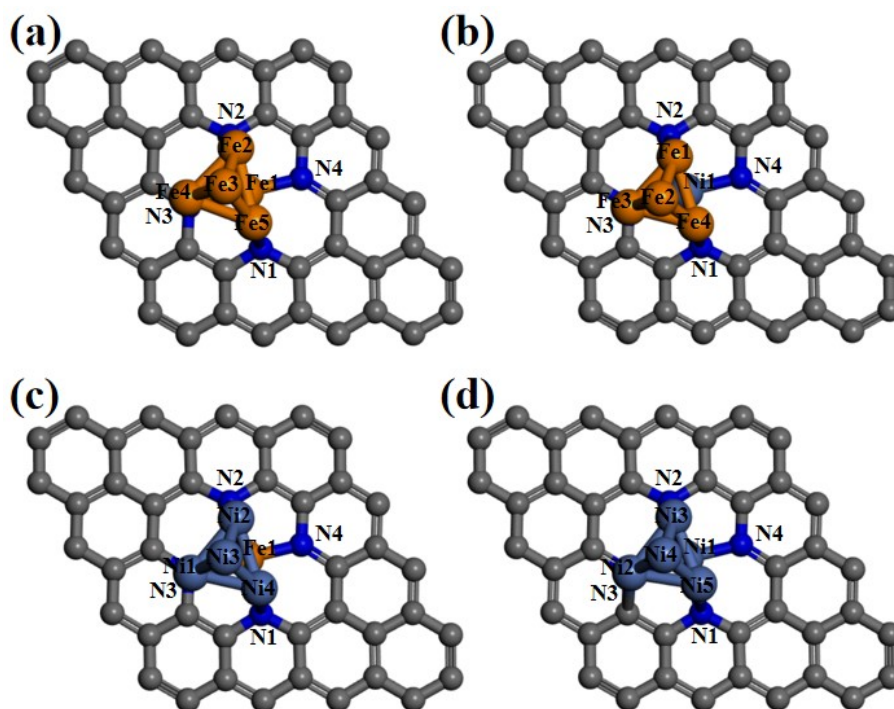


**Figure S5:** Schematic illustration of different adsorption sites on  $M_4$  clusters supported on  $MN_4$ -Gr substrates.

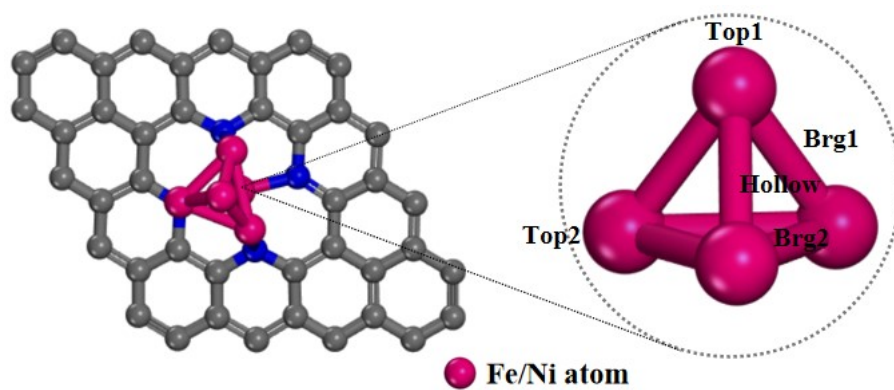


**Figure S6:** The Gibbs free energies of hydrogen adsorption ( $\Delta G_{H^*}$ ) in implicit solvation model.

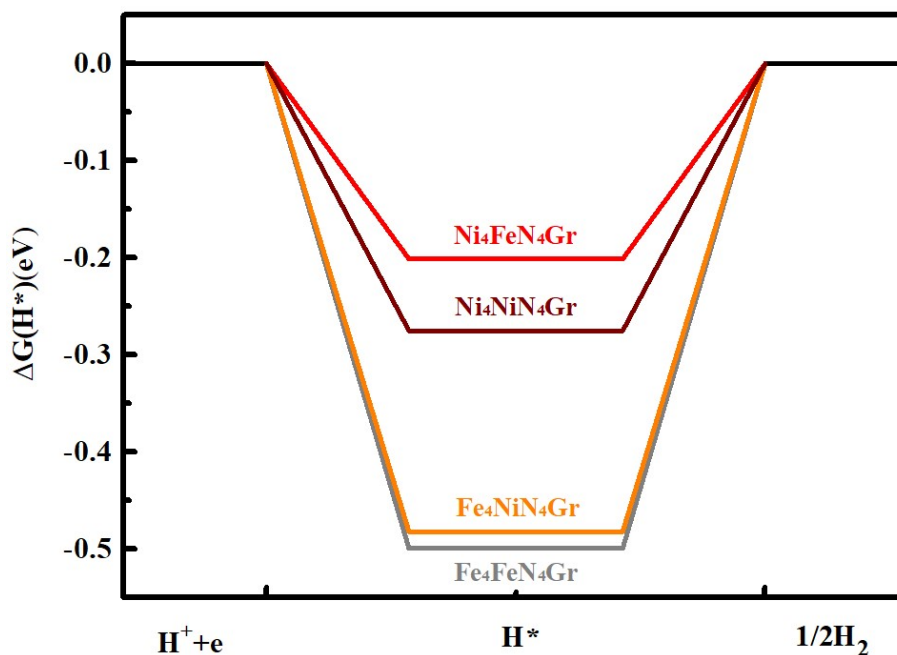


**Figure S7:** Configuration diagrams of the HER mechanism on four model catalysts. (a)-(d) are  $\text{Fe}_4\text{FeN}_4\text{Gr}$ ,  $\text{Fe}_4\text{NiN}_4\text{Gr}$ ,  $\text{Ni}_4\text{FeN}_4\text{Gr}$  and  $\text{Ni}_4\text{NiN}_4\text{Gr}$ , respectively,

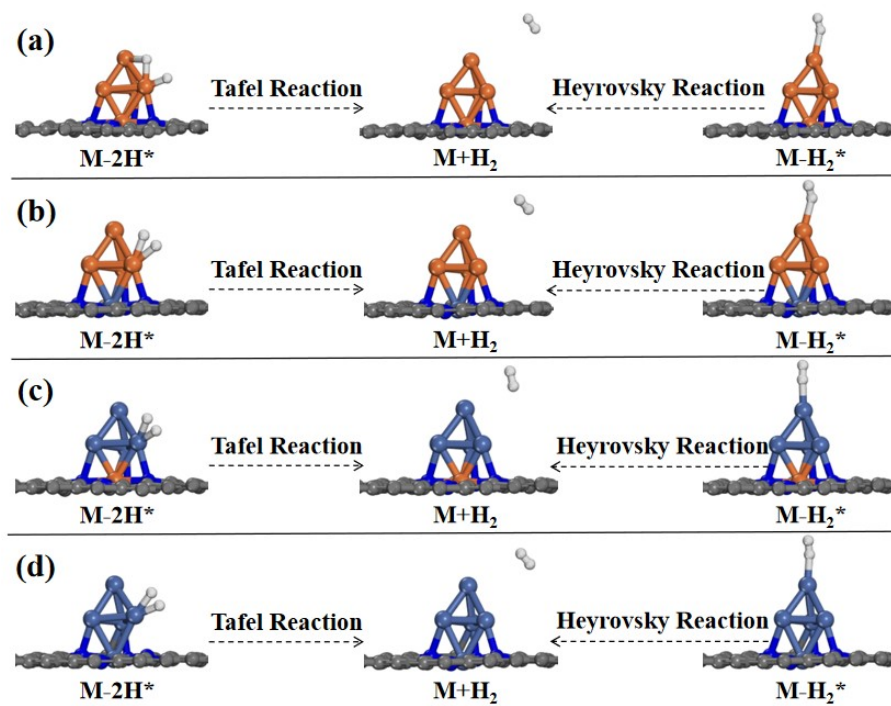


**Figure S8:** The free energy diagrams of HER in implicit solvation model, following the Volmer-Heyrovsky pathway (dotted lines) and Volmer-Tafel pathway (solid lines) on various model catalysts.

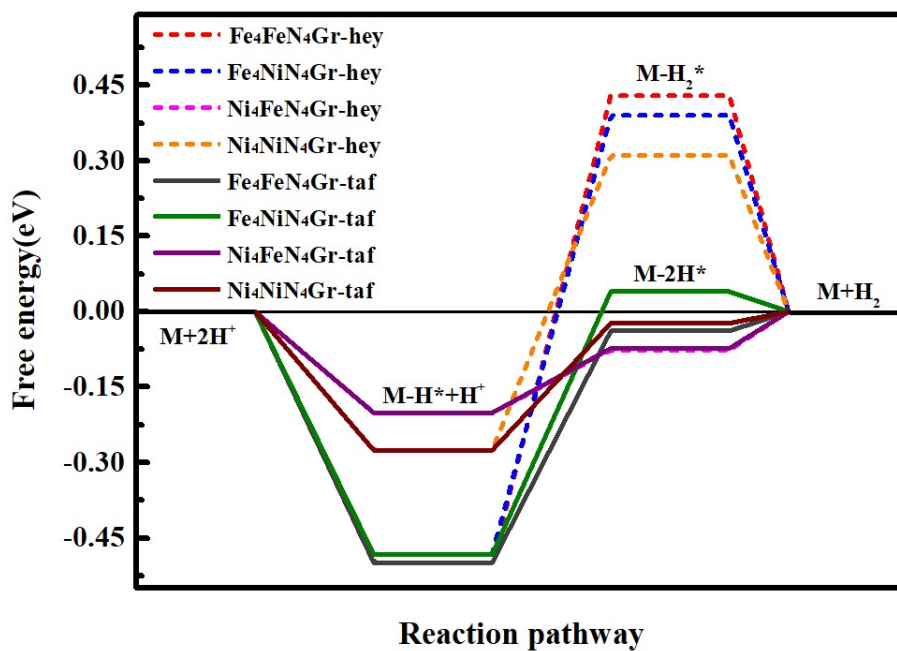


**Figure S9:** Configuration diagram of two hydrogen atoms adsorbed on the  $M_4@MN_4$ -Gr catalyst.

